Journal of Functional Materials and Applied Engineering

Research Paper

Phosphomolybdic Acid-Fe_3O_4 Modified Sludge-Biochar with Tetracycline Adsorption Properties

Giang Fanaei[1], Marwa Piekacz[2], Loan Meath[2,*]

[1] Department of Chemical Engineering, Faculty of Engineering, Center of Excellence in Particle and Material Processing Technology, Chulalongkorn University, Bangkok 10330, Thailand
[2] Jan Kochanowski University, Institute of Chemistry, Uniwersytecka 7, Kielce 25-406, Poland
*Corresponding author: Lo.Meath@interia.pl

Abstract. To address the pressing issue of antibiotic contamination in wastewater, this study developed a novel phosphomolybdic acid (PMA)-Fe_3O_4 ball-milled co-modified sludge-based biochar (PFBC) for tetracycline (TC) removal. Using waste-activated sludge as a precursor, the PFBC composite was synthesized via low-temperature pyrolysis followed by sequential PMA functionalization and mechanochemical Fe_3O_4 incorporation. Comprehensive characterization confirmed that this co-modification strategy successfully enhanced the material's specific surface area, pore volume, and the concentration of surface oxygen-containing functional groups while incorporating magnetic nanoparticles. Batch adsorption tests demonstrated that PFBC exhibited excellent TC sequestration performance, achieving 88.7% removal under optimal conditions (30 mg/L TC, 0.25 g/L PFBC, pH 7). The adsorption followed the Langmuir isotherm and pseudo-second-order kinetic models, with a maximum theoretical capacity of 500.0 mg/g at 25°C. Furthermore, PFBC showed good practical utility with easy magnetic separation (saturation magnetization: 18.1 emu/g) and maintained over 63.3% removal efficiency after five adsorption-desorption cycles.

Keywords: *Sludge biochar; Ball milling; Co-modification; Tetracycline; Adsorption*

Received on 22 March 2023, Accepted on 01 June 2023, Published on 28 July 2023

1 Introduction

According to statistics, China's annual antibiotic production is about 210,000 tons, most of which is applied in livestock breeding and the pharmaceutical industry. Owing to their recalcitrant biodegradation properties, antimicrobial agents persistently enter aquatic and terrestrial ecosystems via municipal and industrial effluent discharge. These contaminants have subsequently been identified in lentic systems, aquifers, and benthic substrates. Environmental persistence of residual antimicrobials can impede autotrophic proliferation, compromise aquatic organismal viability, perturb microbial assemblage composition, and potentially facilitate horizontal transfer of antimicrobial resistance determinants through trophic networks, thereby engendering protracted ecological and public health ramifications.

Therefore, researching and developing efficient methods for antibiotic removal from the environment is crucial.Currently, methods for removing antibiotic pollutants from the environment include membrane separation, advanced oxidation, electrochemical treatment, microbial treatment, and adsorption. Among these decontamination approaches, adsorption stands out owing to superior efficacy, operational simplicity, and economic viability. Diverse adsorptive materials, encompassing activated carbon, carbon nanotubes, and graphene, have been employed for the elimination of contaminants from aqueous systems. However, due to the high cost, poor dispersion, or adsorption performance of these materials, their practical engineering application is limited to some extent. In contrast, biochar, with its abundant raw materials, low cost, and environmental friendliness, has become an ideal biomass adsorbent. Biomass feedstocks suitable for biochar production encompass agricultural and forestry residues, municipal solid waste, woody biomass, animal manure, and sewage sludge. Municipal sludge serves as a cost-effective, organic-rich feedstock for biochar synthesis, simultaneously mitigating secondary pollution concerns through resource valorization. This carbonaceous

adsorbent effectively sequesters diverse contaminants including heavy metals, dyes, phenolic compounds, and inorganic salts. Enhanced sorptive capacity is achievable through chemical or physical surface modification. Oxidative functionalization proves particularly effective by introducing oxygen-containing groups onto the carbon framework. Conventional oxidizing agents include potassium hydroxide, potassium permanganate, nitric acid, hydrogen peroxide, and phosphomolybdic acid (PMA), with PMA demonstrating superior oxidative potential and acidic properties that facilitate biomass conversion and surface oxygenation. Embedded phosphorus and molybdenum species within the biochar matrix may further enhance adsorption performance. Low-temperature PMA modification (200°C) maximizes adsorption capacity while minimizing energy consumption and thermal emissions. High-energy ball milling represents an environmentally friendly, cost-effective, and scalable physical modification technique that reduces particle size to nanoscale, thereby increasing specific surface area, uniformity, and surface functional group density. Additionally, this mechanochemical approach enables direct incorporation of magnetite (Fe_3O_4) nanoparticles without solvent requirements, producing magnetic biochar with improved magnetic separability and reusability. Despite individual efficacy of oxidative or ball milling modifications, research on combined Fe_3O_4-ball milling-oxidative co-modification strategies remains limited. This investigation utilized sewage Sludge as the biochar precursor, with tetracycline (TC) serving as the model antibiotic contaminant. Phosphomolybdic acid (PMA) was employed as the oxidative surface modifier. The PFBC composite was synthesized via low-temperature (200°C) pyrolysis followed by mechanochemical incorporation of Fe_3O_4.

The structural and physicochemical attributes of both unmodified and modified biochar materials were systematically investigated in this work. Its tetracycline sequestration efficacy was subsequently assessed. Through integration of sorption kinetics, equilibrium isotherm data, and comparative characterization of pre- and post-adsorption materials, the underlying mechanism governing tetracycline uptake by PFBC was comprehensively elucidated.This investigation seeks to establish a viable, energy-efficient biochar modification methodology for enhancing sorption performance, concurrently offering novel theoretical underpinnings and technical guidance for sludge valorization.

2. Materials and Methods

2.1 Biochar Preparation

The residual sludge powder was transferred to a tubular furnace, ramped to 200°C at 5°C/min under nitrogen flow (0.1 L/min), and pyrolyzed for 2 h. Subsequent to repeated ultrapure water rinsing until filtrate clarification, the material was desiccated and sieved to yield sludge-derived biochar (BC). A 10 g aliquot of sludge powder was introduced into a dissolved PMA solution.The mixture was subjected to ultrasonic treatment for 1 h, then transferred to a constant-temperature forced-air drying oven until complete desiccation was achieved.The desiccated specimen was transferred to a tubular furnace, ramped to 200°C at 5°C/min under nitrogen flow (0.1 L/min), and pyrolyzed for 2 h. Following ambient cooling, the material underwent repeated ultrapure water rinsing until filtrate clarification, subsequent desiccation, and sieving to yield PMA-functionalized sludge-derived biochar (PBC).

PBC and Fe_3O_4 were combined at a 3:1 mass ratio, then transferred to an agate ball mill jar with grinding media at a 1:100 material-to-ball ratio.The milling operation was conducted at 500 rpm for durations ranging from 1 to 6 hours, with the rotational direction reversed every 30 minutes. The resulting composite material was designated as PFBC.

2.2 Characterization and Analysis

The surface microstructure of biochar specimens was investigated via TEM. Elemental spatial distribution was characterized using energy dispersive spectroscopy (EDS, JED-2300T). porosity was quantified through Brunauer–Emmett–Teller nitrogen adsorption-desorption analysis (ASAP 2460, Micromeritics). Granulometric distribution was assessed via laser diffraction particle size analysis (LPSA, BetterSize2600). The organic elemental constituents (C, H, O, N, S) were quantified employing an elemental analyzer (EA, Vario EL cube, Elementar). Molybdenum and iron concentrations were determined through ICP-OES. Crystallographic phase identification was conducted via X-ray diffraction. Surface elemental composition and chemical speciation were examined

using XPS. Surface functional moieties and chemical architectures were characterized via FTIR. Electrokinetic properties were assessed through nanoparticle tracking and zeta potential determination (ZP, Zetasizer NANO ZS 90 Malvern). Magnetic characteristics were quantified employing a vibrating sample magnetometer (VSM, Lake Shore 7410).

2.3 Adsorption of Tetracycline by Sludge-Based Biochar

Sorption characteristics of BC, PBC, and PFBC prepared via varying ball milling durations (1–6 hours) were systematically investigated for tetracycline (TC) removal. For kinetic investigations, 20 mg of PFBC was added to 100 mL of 30 mg/L tetracycline solution in 250 mL containers, then agitated at 195 rpm in a thermostated orbital shaker for 24 h. Equilibrium TC concentrations were determined via absorbance measurements.

Batch sorption experiments were conducted using 25 mg PFBC dispersed in 100 mL of 30 mg/L TC solution, placed in 250 mL vessels, and agitated at 195 rpm for predetermined intervals. Samples were collected at 0–24 hour intervals to measure absorbance and calculate TC concentration at time t. The effects of adsorbent dosage (0.05–1.10 g/L), solution pH (3–11), and coexisting ions (HCO_3^-, CO_3^{2-}, NO_3^-, SO_4^{2-}, Na^+, NH_4^+, Mg^{2+}, Ca^{2+}) on PFBC sorption performance for TC were systematically investigated. All experiments were conducted at ambient temperature with at least two replicate sets.

2.4 Adsorption Kinetics

For isotherm investigations, 25 mg of PFBC was dispersed in 100 mL TC solution at varying concentrations (10, 30, and 50 mg/L). The mixture was subjected to orbital agitation at 195 rpm within a thermostated shaker to facilitate sorption. Aliquots were withdrawn at designated temporal intervals spanning 0–24 h, subsequently analyzed, and residual tetracycline concentration was quantified.All experimental procedures were performed under ambient thermal conditions (25°C) with duplicate parallel assays. The resultant data were subsequently analyzed and modeled using pseudo-first-order and pseudo-second-order kinetic equations.

2.5 Adsorption Isotherms

For equilibrium isotherm studies, 25 mg of PFBC was introduced into 100 mL of tetracycline solution spanning a concentration gradient of 10–800 mg/L.The mixture was subjected to orbital agitation within a thermostated shaker at 25°C, 35°C, and 45°C, respectively, for 24 h, with duplicate parallel assays conducted.The resultant experimental data were modeled employing Langmuir and Freundlich equilibrium isotherm equations.

2.6 Regeneration Experiment

Subsequent to sorption, PFBC was immersed in absolute ethanol and subjected to ultrasonic treatment under ambient thermal conditions for 1 h, followed by an additional 1 h sonication with fresh absolute ethanol to ensure complete desorption.Magnetic recovery was subsequently employed to isolate the solid phase, which was then desiccated in a thermostated forced-air oven maintained at 65°C for preservation. Regeneration efficacy was evaluated by quantifying the tetracycline sequestration performance of the recovered material: specifically, 25 mg of regenerated biochar was dispersed in 30 mg/L tetracycline solution, subjected to continuous agitation for 24 h, followed by spectrophotometric determination of residual contaminant concentrations in the filtrate. This Adsorption-regeneration protocol was executed iteratively for five cycles under consistent experimental settings.

3. Results and Discussion

3.1 Properties of Modified Sludge-Based Biochar

3.1.1 Surface Morphology

The surface morphology of BC, PBC, and PFBC was investigated using SEM, TEM, and EDS element mapping. As shown in Fig. 1, BC has fewer pore structures and a relatively smooth surface [Fig. 1(a), (d)]. PBC surface shows flaky substances, and the structure is more loose and porous [Fig. 1(b), (e)]. In contrast, the PFBC surface has some protrusions, is rougher, and has more fine particles and black aggregates [Fig. 1(c), (f)]. The irregular surface

topography enhances the specific surface area (SSA) of biochar while augmenting the density of available sorption sites. The irregular surface topography enhances the SSA of biochar while augmenting the density of available sorption sites.

Table 1 EDS Elemental Analysis of Biochars

Sample	Parameter	O	Si	P	Ca	Fe	Mo
BC	Mass fraction / %	64.0	31.2	1.6	0.3	0.9	2.0
	Atomic fraction / %	76.9	21.3	1.0	0.3	0.1	0.4
PBC	Mass fraction / %	52.5	20.8	7.3	1.6	5.9	11.9
	Atomic fraction / %	72.5	16.3	5.2	0.9	2.4	2.7
PFBC	Mass fraction / %	41.5	8.3	2.8	0.9	38.0	8.5
	Atomic fraction / %	68.8	7.8	2.4	0.5	18.1	2.4

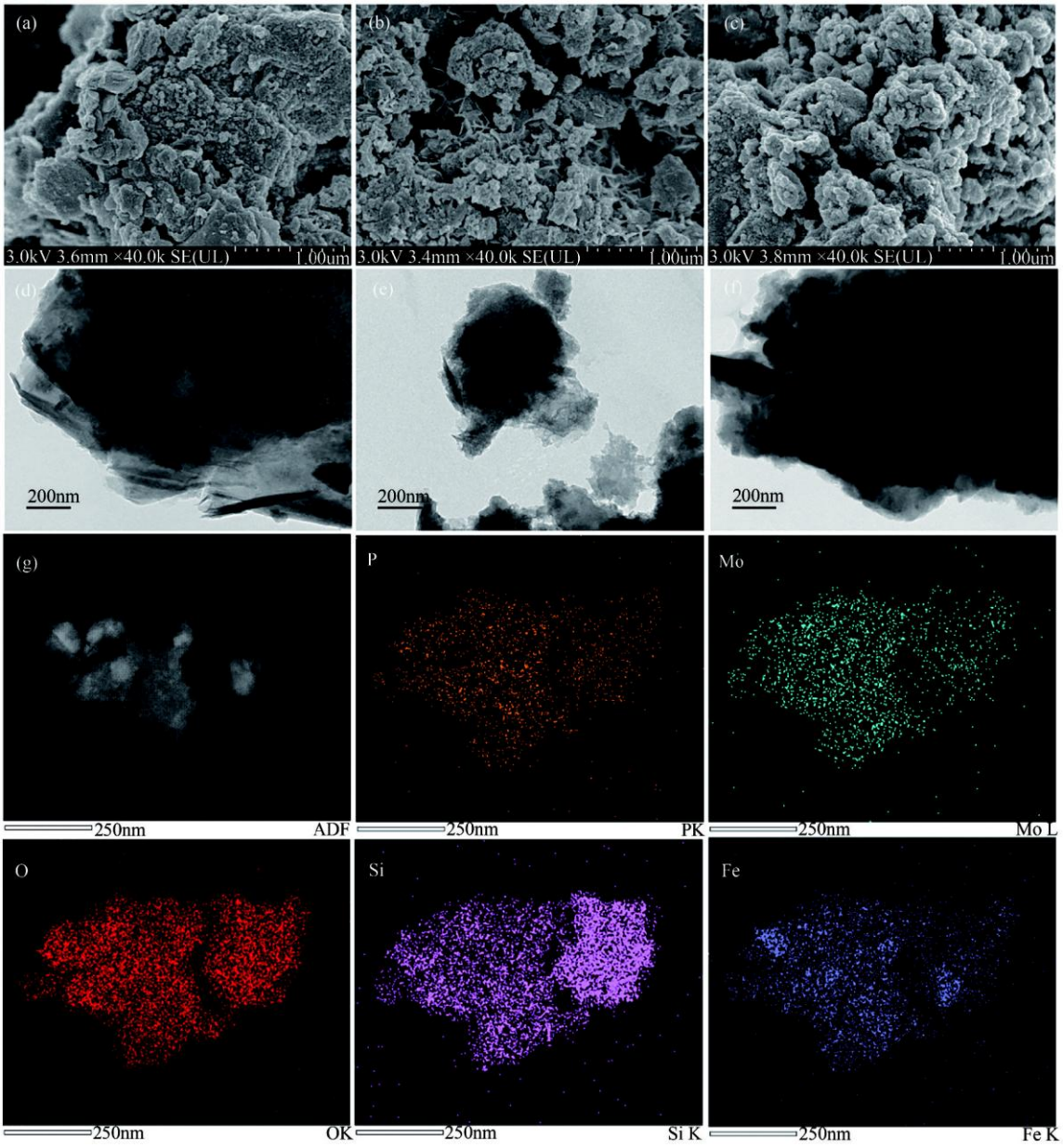

Figure 1 SEM images of BC (a), PBC (b), and PFBC (c), TEM images of BC (d), PBC (e), and PFBC (f), and elemental mapping of PFBC (g)

Porosity of the fabricated samples were probed via BET methodology, with tabulated parameters listed in Table 2. Mean pore diameters of 27.5 nm, 13.3 nm, 18.6 nm, and 13.5 nm were recorded for BC, FBC (ball-milled sludge-derived biochar), PBC, and PFBC respectively, placing all four within mesoporous classification. SSA improvements were observed in FBC and PBC versus untreated BC, indicating that both mechanical attrition and PMA anchoring effectively boost surface development. PFBC surpassed all variants with 56.1 m^2/g—a dramatic upsurge from BC (17.2 m^2/g), FBC (41.1 m^2/g), and PBC (39.1 m^2/g)—while also demonstrating superior pore volume. These enriched structural attributes supply numerous active locations for binding, thus strengthening expected decontamination performance. Additionally, FBC and PFBC underwent size diminishment from micro- to nanoscale, demonstrating that milling operations successfully advance particle consistency and suspension stability. Such data collectively verify pronounced enhancement of the biochar's material properties.

Table 2 Porosity of resultant Biochar samples

Sample	SSA / $m^2 \cdot g^{-1}$	Pore Volume / $cm^3 \cdot g^{-1}$	Average Pore Diameter / nm	Average Particle Size
BC	17.2	0.04	27.5	67.4 μm
FBC	41.1	0.05	13.3	417.4 nm
PBC	39.1	0.13	18.6	110.8μm
PFBC	56.1	0.14	13.5	439.5nm

3.1.2 Composition and Elemental Analysis of Biochar

The crystalline composition of the prepared biochar specimens was analyzed utilizing XRD. From the XRD patterns of biochar (Fig. 2), distinct SiO_2 (PDF#78-1253) characteristic diffraction peaks at 2θ = 20.8°, 26.5°, 50.1°, and 68.1° are observed in BC, PBC, and PFBC. BC, PBC, and PFBC all show Fe_3O_4 diffraction peaks at 2θ = 35.3° and 42.5°. The weak Fe_3O_4 diffraction peaks in BC and PBC may be due to a small amount of Fe_2O_3 naturally present in the sludge being reduced to a small amount of Fe_3O_4 under anaerobic pyrolysis conditions. However, the peak intensity of the Fe_3O_4 (PDF#77-1545) diffraction peak at 2θ = 35.3° in PFBC is significantly enhanced, and new Fe_3O_4 diffraction peaks appear at 2θ = 30.0° and 62.4°, indicating that Fe_3O_4 is successfully introduced into PFBC. Furthermore, the SiO_2 diffraction peak in PFBC is significantly weakened, which is due to the reduced mass proportion of SiO_2 in the biochar after introducing Fe_3O_4. The above results indicate that Fe_3O_4 is successfully loaded onto PFBC via the ball milling modification.

Table 3 Elemental Composition Analysis of Biochars

	Mass Fraction / %						Atomic Ratios		
	C	H	O	N	Mo	Fe	H/C	O/C	(O+N)/C
BC	14.8	2.5	25.6	1.4	0.0	2.4	0.17	1.73	1.82
PBC	13.4	2.0	24.8	1.2	5.9	1.6	0.15	1.85	1.94
PFBC	10.1	2.2	19.7	1.8	2.6	17.5	0.22	1.95	2.13

To further analyze the elemental composition of biochar samples, organic elemental analysis was performed on BC, PBC, and PFBC (Table 3), where the relative proportions of Mo and Fe elements were measured by ICP.As presented in Table 3, PFBC exhibits a reduced H/C ratio relative to both BC and PBC, signifying enhanced aromatic character and structural stability. Conversely, elevated atomic ratios of O/C and (O+N)/C were observed, suggesting intensified hydrophilic character and polar nature for the biochar subjected to combined PMA-Fe_3O_4 modification via ball milling. A higher O/C also indicates more types and greater abundance of functional groups. The above results indicate that PFBC possesses superior adsorption performance. The appearance of Mo elements in PBC and PFBC indicates the successful modification of biochar by PMA, and the significantly higher Fe element content in PFBC compared to BC and PBC further indicates that Fe_3O_4 is loaded onto PBC after ball milling modification.

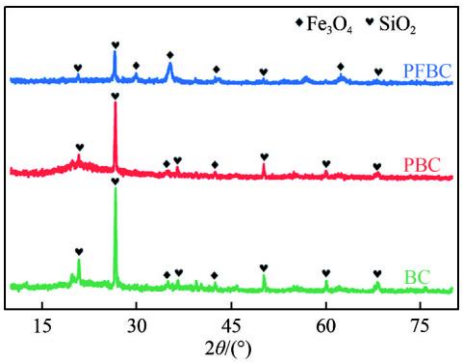

Figure 2 XRD pattern of biochar sample

Table 4 XPS Spectral Analysis of Biochars

Binding Energy / eV	**Characteristic Peak**	Percentage/%		
C 1s		BC	PBC	PFBC
284.8	C-C	60.6	58.5	43.5
286.1	C-OH	19.2	19.5	19.5
286.8	C-O-C	7.2	8.8	14.2
287.8	C=O	6.0	6.4	7.9
288.7	O-C=O	7.0	6.8	14.9
O 1s				
530.9	Fe-O	42.3	40.1	44.0
531.8	C-O	32.2	35.3	26.8
533.1	C=O	25.5	24.6	29.2
Fe 2p				
711.1/724.1	Fe(II)	59.6	60.2	63.6
713.5/726.5	Fe(III)	40.4	39.8	36.4

XPS spectroscopy was employed for comprehensive investigation of the surface chemical constitution of the biochar specimens. As illustrated in Figure 3, the C 1s photoelectron spectra for all three biochar variants exhibit five distinct peak groups. Based on the XPS C 1s spectral analysis presented in Table 4, PBC exhibits a higher oxygen-containing functional group content (41.5%) compared to pristine BC (39.4%), indicating that PMA oxidation successfully introduced additional oxygenated surface moieties. The surface oxygen-containing functional group content of PFBC (56.5%) substantially exceeds that of both pristine BC and PBC. The surface oxygen-containing functional group content of PFBC increases significantly following PMA-Fe_3O_4 ball milling co-modification. The O 1s region of biochar samples (Fig. 3) displayed three distinct contributions at ascending binding energies: Fe-O bonds at 530.9 eV, C-O linkages at 531.8 eV, and carbonyl C=O moieties at 533.1 eV. Quantitative analysis (Table 4) revealed superior Fe-O abundance in PFBC compared to both PBC and BC, substantiating effective integration of magnetite (Fe_3O_4) within the carbonaceous framework. The Fe 2p spectra of biochar samples reveal satellite peaks positioned at 717.2 eV and 730.6 eV, alongside characteristic doublets at 713.5 eV/726.5 eV attributable to Fe(III) and 711.1 eV/724.1 eV corresponding to Fe(II). Quantitative evaluation demonstrates that PBC contains Fe(III) and Fe(II) in proportions of 39.8% and 60.2% respectively, whereas PFBC exhibits an altered distribution of 36.4% Fe(III) and 63.6% Fe(II). The elevated Fe(II) proportion detected in PFBC following modification serves as additional evidence confirming effective immobilization of Fe_3O_4 onto the biochar substrate.

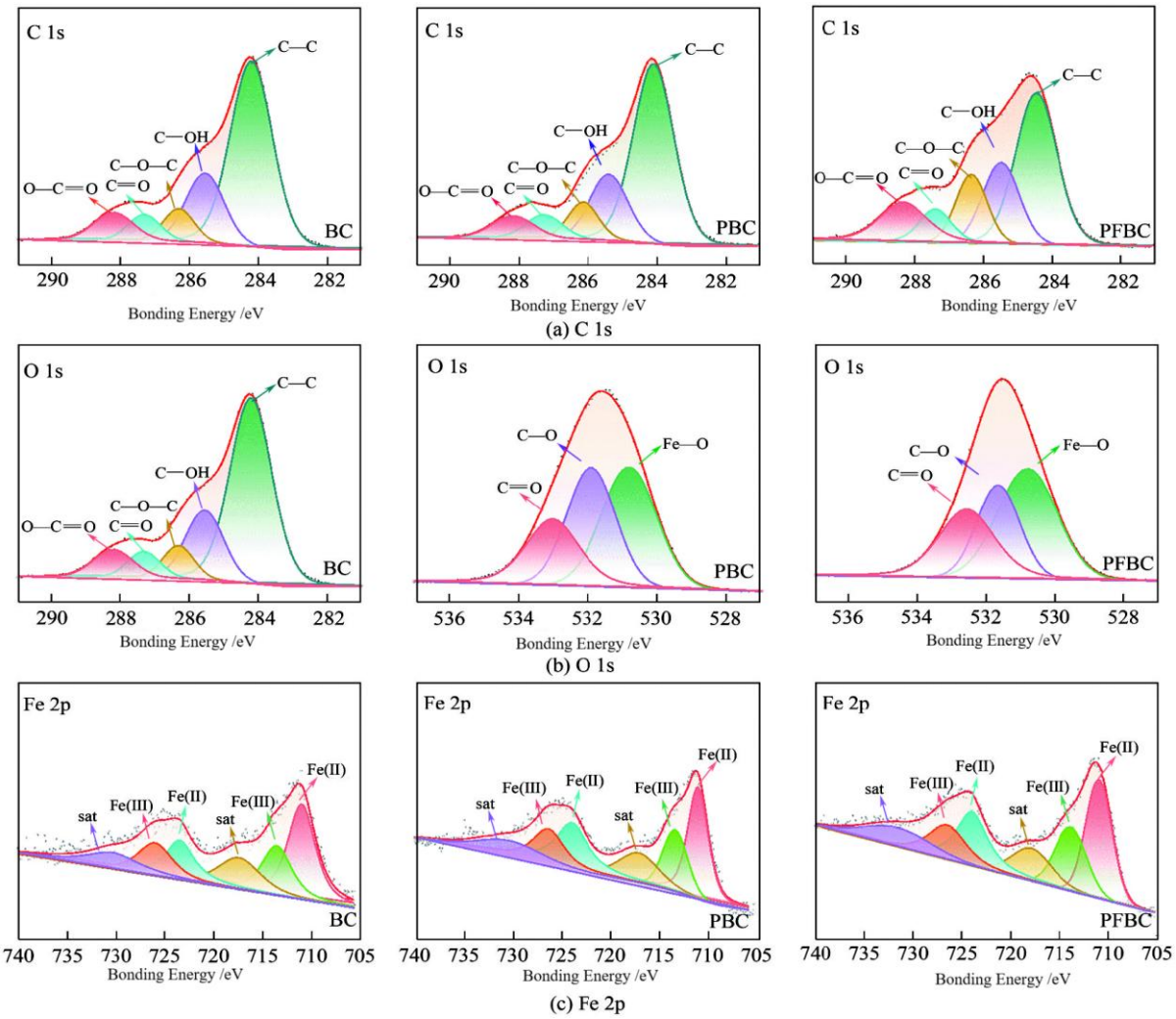

Figure 3 High resolution XPS spectra of biochar samples C 1s, O 1s, and Fe 2p

3.2 TC Adsorption to Biochar

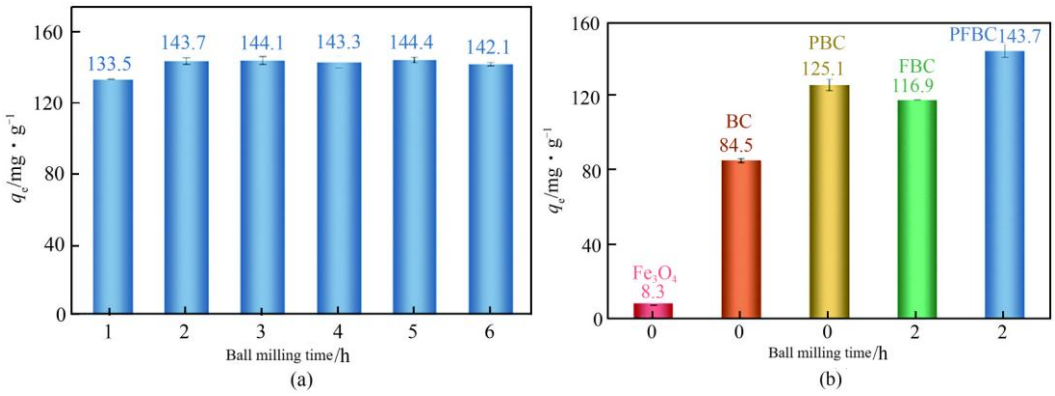

Figure 4 Adsorption capacity of PFBC (a) and different types of adsorbents (b) for TC at different ball milling times

Fig. 4(a) shows the adsorption effect of PFBC ball-milled for 1-6 h on TC. Observation indicates that at a ball milling duration of 1 h, PFBC attained a tetracycline sequestration capacity of 133.5 mg/g. Extending the

mechanochemical treatment duration further, PFBC achieved an enhanced tetracycline uptake capacity of 143.7 mg/g at a ball milling interval of 2 h.Nevertheless, extending mechanochemical treatment beyond 2 h yielded marginal enhancement in tetracycline sequestration capacity. Balancing sorption performance against energy expenditure, the optimal ball milling duration for PFBC preparation was established at 2 h. The tetracycline uptake efficacy of Fe_3O_4, BC, FBC, PBC, and PFBC was subsequently evaluated independently, as illustrated in Fig. 4(b). Following 2 h of mechanochemical treatment (FBC), tetracycline sequestration capacity markedly surpassed that of unmodified biochar, presumably due to enhanced SSA and diminished particle size (Table 2).PBC demonstrated markedly superior tetracycline sequestration relative to BC, arising from concurrent enhancement of SSA and enrichment of surface oxygen-containing functional moieties.The tetracycline sequestration capacities of Fe_3O_4 and PBC were determined at 7.2 mg/g and 124.0 mg/g, respectively, whereas the composite PFBC attained an enhanced uptake of 142.6 mg/g. This phenomenon is attributable to the co-modified PFBC possessing enhanced SSA, augmented pore volume, diminished particle dimensions, and greater abundance of surface functional moieties.

3.3 Effect of Reaction Conditions on TC Adsorption by PFBC

3.3.1 Adsorbent Dosage

The relationship between PFBC dosage and TC removal is presented in Fig. 5(a). Gradual increase in adsorbent quantity drives steady improvement in elimination efficiency, stemming from expanded availability of binding locations. Maximum benefit-cost ratio occurs at 0.25 g/L, where 88.7% removal is realized. Further dosage elevation, despite continued TC elimination enhancement, demonstrates attenuated improvement rates attributable to adsorbent aggregation. Economic optimization considerations similarly supported 0.25 g/L selection for subsequent experimental work.

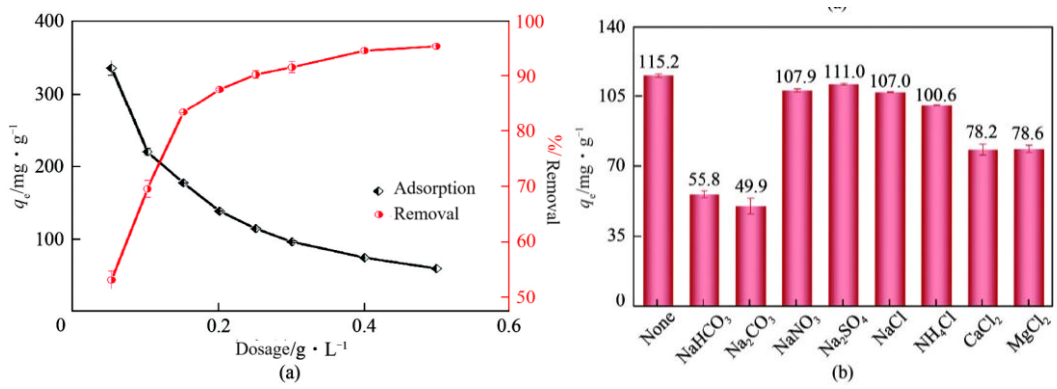

Figure 5 Effects of PFBC dosage (a) and coexisting ions (b) on TC adsorption

3.3.2 Coexisting Ions in Solution

Beyond target contaminants, real wastewater matrices invariably harbor diverse coexisting ionic species. Consequently, the perturbation effects of such ions on PFBC-mediated TC sequestration were systematically examined [Fig. 5(b)].Under pristine conditions devoid of ionic interference, PFBC exhibited a TC uptake capacity of 115.2 mg/g.Upon introducing 0.1 mol/L of HCO_3^-, CO_3^{2-}, NO_3^-, and SO_4^{2-} into the TC solution, the respective sorption capacities diminished to 55.8 mg/g, 49.9 mg/g, 107.9 mg/g, and 111.0 mg/g.This is because adding HCO_3^-, CO_3^{2-} and other ions will increase the solution pH due to hydrolysis, making it alkaline, The addition of HCO_3^- and CO_3^{2-} ions elevates solution pH through hydrolysis, creating alkaline conditions that promote formation of TCH^- and TCH^{2-} species. These develop electrostatic repulsion with the adsorbent surface, diminishing PFBC's tetracycline uptake capacity. Furthermore, NO_3^- and SO_4^{2-} anions may competitively bind to tetracycline molecules or occupy active surface sites on PFBC, further reducing adsorption efficiency. Sodium ions exert minimal suppression on adsorption capacity, whereas magnesium and calcium ions significantly impair tetracycline uptake. This may be because high-concentration, high-valent cations have stronger competitive adsorption with TC, occupying more adsorption sites, leading to reduced adsorption capacity. Although NH_4^+ is not high-valent, due to the high electronegativity of the N element, it may produce competitive adsorption with the $-NH_2$ on TC on PFBC, also having a certain inhibitory effect on TC adsorption.

3.3.3 Solution pH

As an amphoteric molecule, the pKa values of tetracycline are 3.3, 7.7, and 9.7, respectively. At pH values below 3.3, the predominant species is TCH_3^+; within the range of 3.3 to 7.7, TCH_2^o dominates; between 7.7 and 9.7, TCH^- becomes the primary form; and at pH exceeding 9.7, TC^{2-} prevails as the main existing species. pH-modulated sorption behavior is visualized in Fig. 6(a), with PFBC surface charge characteristics provided in Fig. 6(b). The material's point of zero charge registers at pH 5.82. In strongly acidic solution (pH 3), electrostatic repulsion between positively charged adsorbent and cationic tetracycline (TCH_3^+) obstructs interfacial contact. Near the isoelectric point (pH 5), diminished charge-mediated interference between cationic PFBC and zwitterionic tetracycline (TCH_2^o) enables favorable sequestration. Under weakly alkaline conditions (pH 7–9), electrostatic repulsion develops between negatively charged PFBC and anionic tetracycline (TCH^-), attenuating uptake. In strongly basic media (pH 11), intense coulombic repulsion between dianionic TC^{2-} and highly negative PFBC drastically impairs binding. Although maximum efficiency occurs at pH 5, satisfactory performance is preserved at pH 7. Weighing optimal sorption against environmental relevance, neutral pH was adopted as the standard operating condition for subsequent studies.

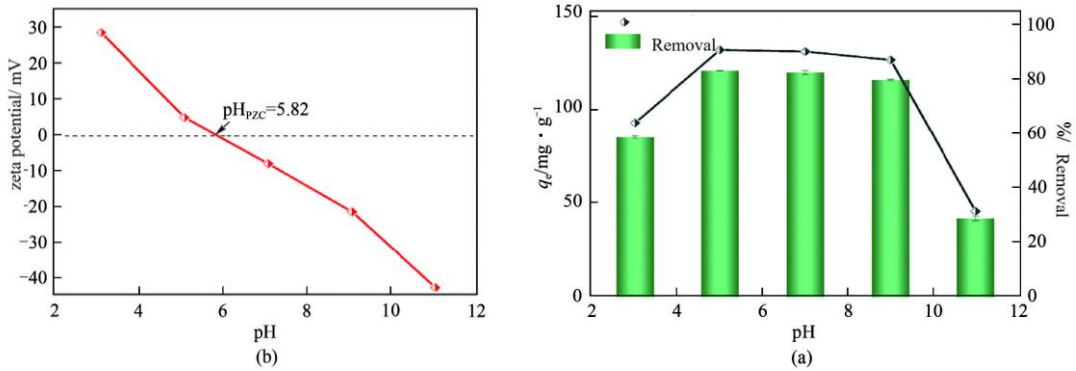

Figure 6 Effect of pH on TC adsorption to PFBC (a) and ζ potential of PFBC (b)

3.4 Analysis of Adsorption Kinetics and Isotherms

Sorption dynamics were assessed at diverse contact durations [Fig. 7(a)], with resultant data modeled employing pseudo-first-order and pseudo-second-order kinetic equations. The derived fitting parameters are compiled in Table 5.The pseudo-first-order formulation generated equilibrium capacity predictions of 23.3, 88.9, and 121.5 mg/g, with corresponding R^2 values of 0.973, 0.985, and 0.960.

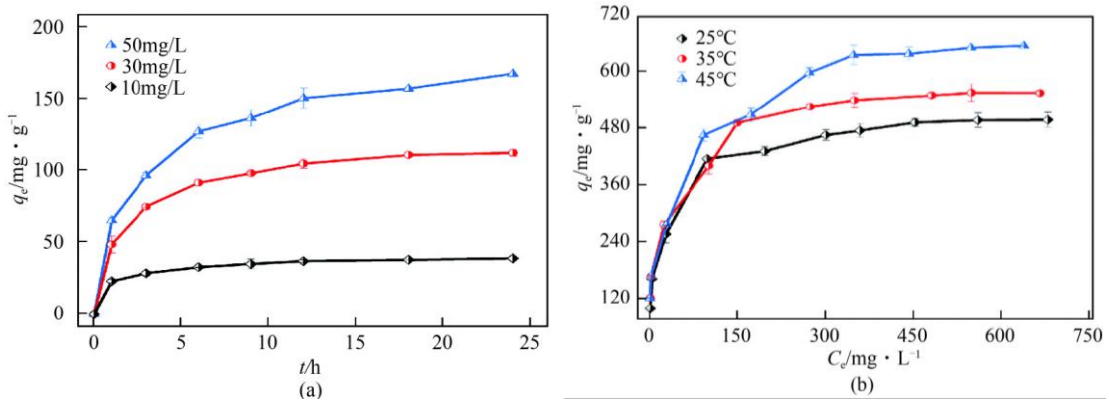

Figure 7 Adsorption kinetics (a) and adsorption isotherm (b) of PFBC

In contrast, the pseudo-second-order approach yielded equilibrium estimates of 38.5, 116.3, and 166.7 mg/g, concomitant with enhanced R^2 coefficients of 0.999, 0.995, and

0.990. Improved statistical correlation and diminished deviation from experimentally observed saturation values confer greater credibility to the pseudo-second-order framework for characterizing PFBC-TC interactions. This comprehensive model subsumes liquid-phase transport, surface complexation, intraparticle penetration, and electronic redistribution steps, distinguishing itself from the pseudo-first-order simplification applicable solely to inception-phase sorption. The compelling alignment with pseudo-second-order behavior implicates chemical bonding as the principal mechanism driving TC immobilization by PFBC.

Table 5 Adsorption Kinetics Fitting Parameters

Fitting Model	Parameter	10 mg/L	30 mg/L	50 mg/L
Adsorption	qe,exp	38.2	112.4	167.7
Pseudo-first-order	qe,cal	23.3	88.9	121.5
	k1	0.279	0.220	0.149
	R^2	0.973	0.985	0.960
Pseudo-second-order	qe,cal	38.5	116.3	166.7
	k2	0.047	0.008	0.003
	R^2	0.999	0.995	0.990

Equilibrium sorption investigations were conducted at 25°C, 35°C, and 45°C across tetracycline concentrations spanning 10 to 800 mg/L to elucidate the correlation between residual concentration and sequestration capacity. The experimental data were modeled employing Langmuir and Freundlich equilibrium isotherm equations, with the derived parameters compiled in Table 6.The Langmuir formulation exhibited R^2 coefficients of 0.999, 0.999, and 0.996, markedly surpassing the Freundlich model's corresponding values of 0.923, 0.952, and 0.974.The superior conformity of the Langmuir formulation, coupled with the strong agreement between theoretical maximum capacities and empirical observations, demonstrates that tetracycline uptake by PFBC adheres to Langmuir behavior—indicative of monolayer coverage on energetically uniform surface sites.Furthermore, Freundlich constants (1/n) below unity substantiate the favorable nature of tetracycline sequestration on PFBC.

Table 6 Adsorption Isotherm Fitting Parameters

Fitting Model	Parameter	298K	308K	318K
Adsorption Capacity	qmax,exp	491.3	548.5	644.2
	qmax,cal	500.0	555.6	666.7
Langmuir	KL	0.035	0.035	0.021
	R^2	0.999	0.999	0.996
	KF	86.05	73.19	80.39
Freundlich	1/n	0.307	0.316	0.340
	R^2	0.923	0.952	0.974

Fig. 7(b) reveals substantial amplification of uptake capacity with progressive elevation in initial TC concentration. The adsorbent realizes peak loading of 500.0 mg/g under 25°C conditions (Table 6). Benchmarking analysis was conducted comparing PFBC's maximum capacity against published data for biochars derived from wastewater sludge and diverse lignocellulosic precursors (Table 7). Despite not attaining the uppermost values documented in existing literature, PFBC nevertheless exhibits markedly enhanced sorption capability relative to the majority of comparable carbonaceous materials.The aforementioned results demonstrate that PFBC functions as an efficient adsorbent with considerable potential for pollutant remediation applications.

Table 7 Saturation Adsorption Capacities of Different Biochars for TC

Raw Material	Modification Method	Saturation Adsorption Capacity / mg/g	Reference
		25°C	35°C
Sludge	H3PO4 · 12MoO3+ Ball milling	500.0	555.6
Sludge	NaOH+Chitosan+ NH4Fe(SO4)2 · 12H2O+ (NH4)2Fe(SO4)2 · 6H2O	184.3	199.3
Sludge	KOH+FeCl2+FeCl3	140.7	141.6
Sludge	ZnCl2+Chitosan+FeSO4 · 7H2O+Na2S · 9H2O	183.0	199.4
Sludge	ZnCl2+FeSO4 · 7H2O+Na2S · 9H2O	174.1	154.6
Papermaking Sludge	Unmodified	125.2	—
Peanut Shell	CaCl2	72.3	—
Orange Peel	MnCl2+FeCl3 · 6H2O+FeCl2 · 4H2O	167.5	—
Straw	KOH	307.8	379.5
Straw	MnCl2	736.0	876.0
Lignocellulose	HCl	1078.9	1901.4

3.5 Adsorption Mechanism Analysis

Biochars inherently feature extensive surface areas and well-developed porosity that support effective contaminant capture through pore-filling processes. Post-adsorption SEM imaging of PFBC (Fig. 8) reveals substantial surface coverage with raised, non-uniform structures, indicating TC molecules access internal carbon pores and subsequently concentrate at the surface. BET analysis comparing native and TC-saturated PFBC (Table 8) demonstrates significant textural alteration: SSA dropped substantially from 56.1 m^2/g to 5.9 m^2/g, while pore volume decreased from 0.14 to 0.03 cm^3/g. These considerable declines in both parameters confirm TC immobilization occurs mainly through pore-filling, with the antibiotic occupying both internal void spaces and external surface areas of the carbon material.

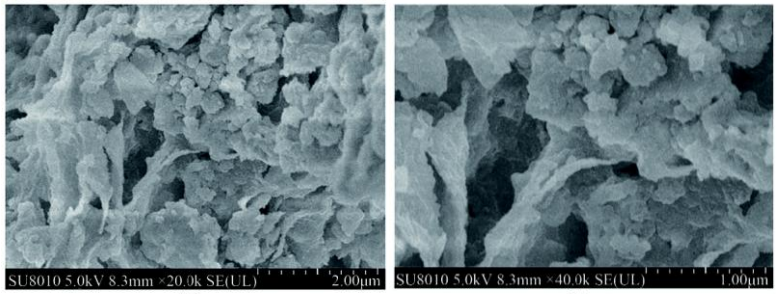

Figure 8 SEM image of PFBC adsorbing TC

Table 8 SSA and Pore Structure Parameters of PFBC Before and After TC Adsorption

Sample	SSA / m2/g	Total Pore Volume / cm3/g	Average Pore Diameter / nm
PFBC	56.1	0.14	13.5
PFBC-TC	5.9	0.03	16.4

After TC adsorption, the binding energy and relative content of XPS C 1s and O 1s changed significantly [Fig. 9(a), (b)]. XPS C 1s spectral modifications following TC exposure indicate π-π interactions between PFBC's aromatic carbon structures and TC molecules. Corresponding O 1s alterations demonstrate oxygenated functional groups contribute to TC removal through hydrogen bonding. These spectral transformations verify hydrogen bond formation between the adsorbent and adsorbate. Iron oxide species additionally serve as coordination sites for TC complexation, supported by Fe-O binding energy shift from 530.9 eV to 531.2 eV and relative mass fraction decrease from 42.9% to 35.1%, confirming metal-ligand coordination.

FTIR spectroscopy [Fig. 9(c)] shows Fe-O stretching vibration displacement from 549 cm^{-1} to 567 cm^{-1}, further

validating metal complexation involvement. Aromatic C=O characteristic peak shift (1656 cm^{-1} → 1672 cm^{-1}) additionally corroborates π-π interactions. The C-O and O-H stretching vibrations initially observed at 1043 cm^{-1} and 3425 cm^{-1}, respectively, exhibited bathochromic shifts to 1055 cm^{-1} and 3447 cm^{-1}, corroborating the involvement of hydrogen bonding interactions mediated by oxygen-containing functional moieties.

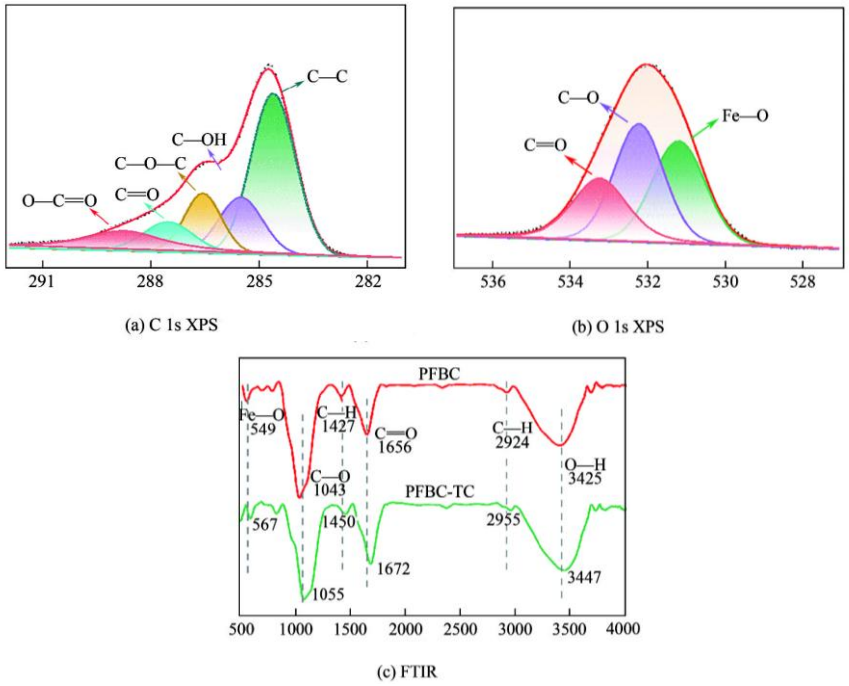

Figure 9 XPS and infrared spectra of PFBC adsorbed TC

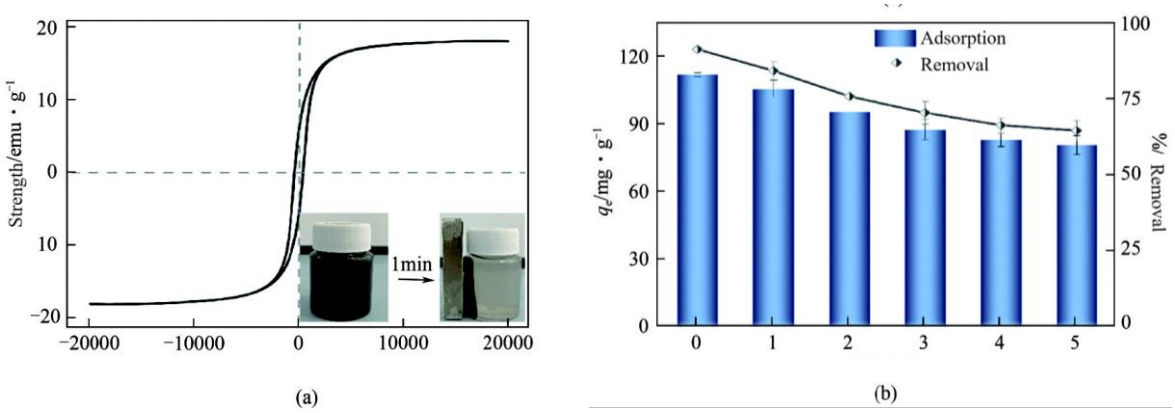

Figure 10 Hysteresis Loop (a) and Reusability (b) of PFBC

3.6 Reusability

PFBC demonstrates saturation magnetization of 18.1 emu/g [Fig. 10(a)], enabling convenient magnetic separation from aqueous solutions through external field application [inset, Fig. 10(a)] to facilitate recovery and reuse. The exhausted adsorbent was retrieved from treated wastewater and subjected to five consecutive adsorption-regeneration cycles. As shown in Fig. 10(b), TC removal efficiency exhibits gradual decline with increasing cycle number, likely resulting from cumulative pore blockage and progressive loss of active binding sites within the PFBC framework. However, after 5 regeneration-adsorption cycles, PFBC can still remove 63.3% of TC from the solution. In summary, PFBC has good reusability.

4. Conclusions

Building upon the promising results of the PFBC adsorbent, several future research directions are recommended to advance its practical application. First, evaluating PFBC's performance in real wastewater matrices is crucial. Future work should test the adsorbent against complex, multi-contaminant streams from sources like pharmaceutical or livestock wastewater to assess its selectivity and robustness under realistic conditions. Second, exploring coupled treatment processes could be valuable. Integrating PFBC adsorption as a pre-concentration step with subsequent advanced oxidation processes (e.g., activation of persulfate by the Fe/Mo species) may achieve complete mineralization of antibiotics, addressing the issue of concentrated adsorbate disposal. Furthermore, optimizing the regeneration strategy is needed to improve the material's long-term economic viability. Investigating alternative, more efficient desorption eluents or thermal regeneration methods could help recover more adsorption capacity over repeated cycles. Finally, scaling up the synthesis protocol for PFBC and conducting techno-economic analyses are essential steps to bridge the gap between laboratory proof-of-concept and field-scale implementation in wastewater treatment plants.

References

[1] ZHENG Huidong. The source of antibiotics in aquatic environment and its impact on human health[J]. Journal of Environmental Hygiene, 2018, 8(1): 73-77.

[2] LIU Qing, ZHONG Lubin, ZHAO Quanbao, et al. Synthesis of Fe3O4/polyacrylonitrile composite electrospun nanofiber mat for effective adsorption of tetracycline[J]. ACS Applied Materials & Interfaces, 2015, 7(27): 14573-14583.

[3] ZENG Zhuotong, YE Shujing, WU Haipeng, et al. Research on the sustainable efficacy of g-MoS2 decorated biochar nanocomposites for removing tetracycline hydrochloride from antibiotic-polluted aqueous solution[J]. The Science of the Total Environment, 2019, 648: 206-217.

[4] QIAO Disi, LI Zehao, DUAN Jinyou, et al. Adsorption and photocatalytic degradation mechanism of magnetic graphene oxide/ZnO nanocomposites for tetracycline contaminants[J]. Chemical Engineering Journal, 2020, 400: 125952.

[5] SUN Hongwei, YANG Jingjie, WANG Yue, et al. Study on the removal efficiency and mechanism of tetracycline in water[J]. Coatings, 2021, 11(11): 1354.

[6] ZHENG Shimei, WANG Yandong, CHEN Cuihong, et al. Current progress in natural degradation and enhanced removal techniques of antibiotics in the environment: A review[J]. International Journal of Environmental Research and Public Health, 2022, 19(17): 10919.

[7] ZHANG Peizhen, LI Yanfei, CAO Yaoyao, et al. Characteristics of tetracycline adsorption by cow manure biochar prepared at different pyrolysis temperatures[J]. Bioresource Technology, 2019, 285: 121348.

[8] MA Yongfei, LI Ming, LI Ping, et al. Hydrothermal synthesis of magnetic sludge biochar for tetracycline and ciprofloxacin adsorptive removal[J]. Bioresource Technology, 2021, 319: 124199.

[9] LIANG Huagen, ZHU Chenxi, JI Shan, et al. Magnetic Fe2O3/biochar composite prepared in a molten salt medium for antibiotic removal in water[J]. Biochar, 2022, 4(1): 3.

[10] ZHANG Qingfa, CAI Hongzhen, YI Weiming, et al. Biocomposites from organic solid wastes derived biochars: A review[J]. Materials, 2020, 13(18): 3923.

[11] LIANG Meina, LU Lin, HE Huijun, et al. Applications of biochar and modified biochar in heavy metal contaminated soil: A descriptive review[J]. Sustainability, 2021, 13(24): 14041.

[12] DAI Xiaohu. Applications and perspectives of sludge treatment and disposal in China[J]. Science, 2020, 72(6): 30-34.

[13] ZHOU Shanlei, XU Yabing, ZHANG Yuxi, et al. Preparation of sludge-based biochar and its adsorption to reactive black 5 dye[J]. Shandong Chemical Industry, 2023, 52(17): 239-241.

[14] HE Dandan, ZHANG Zeyu, LIU Juanli, et al. Application of municipal sludge biochar in wastewater adsorption treatment[J]. Fine Chemicals, 2023(7): 1447-1457.

[15] DEVI Parmila, SAROHA Anil K. Utilization of sludge based adsorbents for the removal of various pollutants: A review[J]. The Science of the Total Environment, 2017, 578: 16-33.

[16] FEI Yongxin, MA Huiqiang, LI Shuang. Study on adsorption performance of modified activated sludge biochar for phenol in water[J]. Journal of Liaoning Petrochemical University, 2022, 42(3): 19-24.

[17] ZHANG Xu, SHU Xin, ZHOU Xiaolin, et al. Magnetic reed biochar materials as adsorbents for aqueous copper and phenol removal[J]. Environmental Science and Pollution Research International, 2023, 30(2): 3659-

3667.
[18] KASERA Nitesh, AUGOUSTIDES Victoria, KOLAR Praveen, et al. Effect of surface modification by oxygen-enriched chemicals on the surface properties of pine bark biochars[J]. Processes, 2022, 10(10): 2136.
[19] HE Xian, HONG Zhineng, JIANG Jun, et al. Enhancement of Cd(II) adsorption by rice straw biochar through oxidant and acid modifications[J]. Environmental Science and Pollution Research International, 2021, 28(31): 42787-42797.
[20] GUO Zijing, CHEN Xin, HANG Jiacheng, et al. Oxidative magnetization of biochar at relatively low pyrolysis temperature for efficient removal of different types of pollutants[J]. Bioresource Technology, 2023, 387: 129572.
[21] LIU Sen, LI Jihui, XU Shuang, et al. A modified method for enhancing adsorption capability of banana pseudostem biochar towards methylene blue at low temperature[J]. Bioresource Technology, 2019, 282: 48-55.
[22] LIN Shenglun, ZHANG Hongjie, CHEN Wei-Hsin, et al. Low-temperature biochar production from torrefaction for wastewater treatment: A review[J]. Bioresource Technology, 2023, 387: 129588.
[23] WU Jingqi, WANG Tongshuai, LIU Yuyan, et al. Norfloxacin adsorption and subsequent degradation on ball-milling tailored N-doped biochar[J]. Chemosphere, 2022, 303(Pt 3): 135264.
[24] HUANG Zhexi, YI Yunqiang, ZHANG Nuanqin, et al. Removal of fluconazole from aqueous solution by magnetic biochar treated by ball milling: Adsorption performance and mechanism[J]. Environmental Science and Pollution Research International, 2022, 29(22): 33335-33344.
[25] SHAN Danna, DENG Shubo, ZHAO Tianning, et al. Preparation of ultrafine magnetic biochar and activated carbon for pharmaceutical adsorption and subsequent degradation by ball milling[J]. Journal of Hazardous Materials, 2016, 305: 156-163.
[26] HE Juan, TANG Jingchun, ZHANG Zheng, et al. Magnetic ball-milled FeS@biochar as persulfate activator for degradation of tetracycline[J]. Chemical Engineering Journal, 2021, 404: 126997.
[27] WEI Zehua, LI Haihong, JIA Miaomiao, et al. NaOH-ball-milled co-modified magnetic biochar and its oil adsorption properties[J]. Particuology, 2023, 83: 40-49.
[28] GUO Tianxiang, ZHANG Yonghe, GENG Yuhan, et al. Surface oxidation modification of nitrogen doping biochar for enhancing CO2 adsorption[J]. Industrial Crops and Products, 2023, 206: 117582.
[29] ZHANG Dawei, HE Qianqian, HU Xiaolan, et al. Enhanced adsorption for the removal of tetracycline hydrochloride(TC) using ball-milled biochar derived from crayfish shell[J]. Colloids and Surfaces A: Physicochemical and Engineering Aspects, 2021, 615: 126254.
[30] CAI Siying, ZHANG Weijun, CHEN Kang, et al. Preparation of Chinese medicine wastes biochar and its adsorption characteristics to tetracycline in water[J]. Safety and Environmental Engineering, 2022, 29(3): 178-186.
[31] MEI Yanglu, XU Jin, ZHANG Yin, et al. Effect of Fe-N modification on the properties of biochars and their adsorption behavior on tetracycline removal from aqueous solution[J]. Bioresource Technology, 2021, 325: 124732.
[32] ZHAO Zhendong, WU Qianqian, NIE Tiantian, et al. Quantitative evaluation of relationships between adsorption and partition of atrazine in biochar-amended soils with biochar characteristics[J]. RSC Advances, 2019, 9(8): 4162-4171.
[33] YANG Hucheng, YU Hao, WANG Jiahao, et al. Magnetic porous biochar as a renewable and highly effective adsorbent for the removal of tetracycline hydrochloride in water[J]. Environmental Science and Pollution Research, 2021, 28(43): 61513-61525.
[34] ZOU Chenglong, WU Qin, NIE Fahui, et al. Application of magnetic porous graphite biochar prepared through one-step modification in the adsorption of tetracycline and ciprofloxacin from aqueous solutions[J]. Waste and Biomass Valorization, 2023, 15(3): 1477-1494.
[35] ZHANG Qingle, WANG Zhong, LI Rui. Adsorption characteristics of tetracycline on biochar from salvia miltiorrhiza[J]. Shandong Chemical Industry, 2022, 51(19): 47-50.
[36] DHIBAR Subhendu, PAL Suchetana, KARMAKAR Kripasindhu, et al. Two novel low molecular weight gelator-driven supramolecular metallogels efficient in antimicrobial activity applications[J]. RSC Advances, 2023, 13(47): 32842-32849.
[37] OULD M'HAMED Mohamed. Ball milling for heterocyclic compounds synthesis in green chemistry: A review[J]. Synthetic Communications, 2015, 45(22): 2511-2528.
[38] SHI Qiyu, WANG Wangbo, ZHANG Hongmin, et al. Porous biochar derived from walnut shell as an efficient adsorbent for tetracycline removal[J]. Bioresource Technology, 2023, 383: 129213.

[39] FAN Shisuo, FAN Xinru, WANG Shuo, et al. Effect of chitosan modification on the properties of magnetic porous biochar and its adsorption performance towards tetracycline and Cu2+[J]. Sustainable Chemistry and Pharmacy, 2023, 33: 101057.
[40] KIM Ji Eun, BHATIA Shashi Kant, SONG Hak Jin, et al. Adsorptive removal of tetracycline from aqueous solution by maple leaf-derived biochar[J]. Bioresource Technology, 2020, 306: 123092.
[41] FAN Shisuo, TANG Jie, WANG Yi, et al. Biochar prepared from co-pyrolysis of municipal sewage sludge and tea waste for the adsorption of methylene blue from aqueous solutions: Kinetics, isotherm, thermodynamic and mechanism[J]. Journal of Molecular Liquids, 2016, 220: 432-441.
[42] QI Liqiang, TENG Fei, DENG Xin, et al. Experimental study on adsorption of Hg(II) with microwave-assisted alkali-modified fly ash[J]. Powder Technology, 2019, 351: 153-158.
[43] ZHANG Juanxiang, ZHAO Baowei, MA Fengfeng, et al. Adsorption characteristics and mechanism of tetracycline by biochars derived from paper industry sludge[J]. China Environmental Science, 2020, 40(9): 3821-3828.
[44] HUANG Hui, GUAN Yingbing, SUN Xuwei, et al. Adsorption behavior of chlortetracycline on the biochar-based magnetic gel balloon[J]. Technology of Water Treatment, 2023, 49(7): 32-37.
[45] LIU Juanli, ZHOU Baiqin, ZHANG Hong, et al. A novel biochar modified by chitosan-Fe/S for tetracycline adsorption and studies on site energy distribution[J]. Bioresource Technology, 2019, 294: 122152.
[46] MA Juan, ZHOU Baiqin, ZHANG Hong, et al. Fe/S modified sludge-based biochar for tetracycline removal from water[J]. Powder Technology, 2020, 364: 889-900.
[47] FAN Fangfang, TONG Zhongkai, ZUO Weiyuan. Study on adsorption of tetracycline from wastewater by calcium modified peanut shell biochar[J]. Inorganic Chemicals Industry, 2023, 55(6): 109-115.
[48] LIN Bingfeng, CHEN Zhihao, YANG Fangli, et al. Adsorption performance of tetracycline by manganese ferrite-modified biochar[J]. Journal of Agro-Environment Science, 2023, 42(7): 1585-1596.
[49] XU Jin, MA Yifan, YAO Guoqing, et al. Effect of KOH activation on the properties of biochar and its adsorption behavior on tetracycline removal from an aqueous solution[J]. Environmental Science, 2022, 43(12): 5635-5646.
[50] ZHAO Zhiwei, CHEN Chen, LIANG Zhijie, et al. Enhanced adsorption activity of manganese oxide-modified biochar for the removal of tetracycline from aqueous solution[J]. Journal of Agro-Environment Science, 2021, 40(1): 194-201.
[51] LI Guoting, LI Kangli, ZHANG Shuaiyang, et al. Comparative study on adsorption of methylene blue and tetracycline by lignocellulosic biochar[J]. Jiangsu Agricultural Sciences, 2021, 49(18): 234-240.
[52] LI Bin, ZHANG Yin, XU Jin, et al. Effect of carbonization methods on the properties of tea waste biochars and their application in tetracycline removal from aqueous solutions[J]. Chemosphere, 2021, 267: 129283.
[53] QU Jianhua, ZHANG Bo, TONG Hua, et al. High-efficiency decontamination of Pb(II) and tetracycline in contaminated water using ball-milled magnetic bone derived biochar[J]. Journal of Cleaner Production, 2023, 385: 135683.
[54] WANG Kaifeng, YAO Runlin, ZHANG Dongqing, et al. Tetracycline adsorption performance and mechanism using calcium hydroxide-modified biochars[J]. Toxics, 2023, 11(10): 841.
[55] LIU Sen. Study on modification of banana pseudostem biochar and its adsorption properties for methylene blue[D]. Haikou: Hainan University, 2020.